Comparison of LES and RANS in numerical simulation of turbulent non-premixed flame under MILD combustion condition

M. Hallaji and K. Mazaheri
kiumars@modares.ac.ir
Department of Mechanical Engineering, Tarbiat Modares University, Tehran, Iran

Abstract
MILD combustion is a recent development in the combustion of hydrocarbon fuels which promises high efficiencies and low NOx emissions. In this numerical study, a turbulent non-premixed CH4+H2 jet flame issuing into a hot and diluted co-flow air is considered to simulate a moderate and intense low oxygen dilution (MILD) combustion regime. This flame is related to the experimental setup of Dally et al. [1]. The numerical simulation is carried out using the Partially Stirred Reactor (PaSR) combustion model, to describe turbulence-chemistry interaction, and a simple mechanism to represent the chemical reactions of Hydrogen/Methane jet flame. In this article the Large Eddy Simulation method (LES) compared with Reynolds Averaged Navier Stocks (RANS) approach in the prediction of flame characteristics. We study the effects of two turbulence models, Smagorinsky and modified standard k-ε model, as basic models in LES and RANS for simulation of MILD combustion. Smagorinsky model has shown a better performance, and it is able to predict more accurate flame characteristics than modified standard k-ε model.

Introduction

The Moderate or Intense Low-oxygen Dilution (MILD) technology, also called flameless combustion, offers great advantages in terms of large energy savings with very low pollutant emissions. From a historical point of view, the technology was first named Excess Enthalpy Combustion [2], while today it is called High Temperature Air combustion (HiTAC), Flameless Oxidation (FLOX) and MILD combustion. In general, the MILD combustion takes place when the temperature of the reactant mixture is higher than the mixture self-ignition temperature (T_{inlet} > Tsi) and when the maximum temperature difference with respect to the inlet temperature is lower than the mixture self-ignition temperature [3]. In the MILD regime fuel is mixed with a diluted and highly pre-heated air to create a distributed reaction zone with a reduced peak temperature. These features produce a uniform temperature field and lower emission of pollutants than conventional non-premixed flame [4]. The conditions of elevated and uniform temperature distribution and low oxygen concentration, lead to slower reaction rates (Damkohler number of the order of unity) and enhances the influence of molecular diffusion on flame characteristics [4].

The experimental studies of MILD combustion provide important data that can also be used for calibrating numerical simulations [e.g., 1-3]. Dally [1] experimentally investigated the effect of oxygen concentration in hot coflow in H_2-CH_4 turbulent non-premixed flame under MILD condition. His results showed that reducing the oxygen mass fraction from 9% to 3% in the hot oxidant stream results in considerable changes to the flame structure. These changes

include a peak temperature drop of up to 400 K and a threefold drop in OH and CO levels. Christo and Dally [4, 5] used Reynolds-Averaging Navier-Stokes approach to model the flow, compositions and temperature fields. Their results indicated the importance of diffusion effects in the numerical prediction of MILD combustion. The weakness of the standard k-ε model in predicting round jet flames was also reported by Dally et al. [4, 5]. They concluded that adjusting the value of the $C_{\varepsilon 1}$ constant in the dissipation rate equation (from 1.44 to 1.6) led to a noticeable improvement in prediction accuracy. They [5] also demonstrated the limitations of conserved scalar based models (e.g. the ξ/PDF and flamelet) under MILD conditions and showed that the eddy dissipation concept (EDC) performs better. The EDC model performed reasonably well for flames with 9% and 6% O2. However the numerical model prediction for 3% O2 was poor. Moreover, their results showed that at 120-mm axial location, the model did not perform well. They suggested that the occurrence of intermittent localized flame extinction, which was not predicted reasonably by their model, could be the reason of this poor prediction [4, 5]. It has been shown that heat release in MILD combustion is controlled by both fluid motion and chemical kinetics [6]. Hence, it seems that the partially stirred reactor (PaSR) model can be a good candidate to assess the extent of turbulence-kinetics interaction in MILD combustion. The PaSR combustion model was developed by Golovitchev [7] in 2000 to simulate the Diesel engines reacting flow field. This model is an extension of the Eddy Dissipation Concept (EDC) that is capable of using a detailed kinetics. Golovichev et al. [8] applied detailed kinetics and the Partially Stirred Reactor concept (PaSR) to describe the turbulence/chemistry interaction in Flameless combustion. His Simulation results clearly illustrated that the flame structure is significantly affected by oxygen concentration [8].

High-fidelity simulations of non-premixed turbulent combustion regimes requires an accurate description of the fuel and oxidizer mixing that cannot be achieved under steady assumptions (RANS). Large-eddy simulation (LES) of turbulent combustion has attracted more and more attention. There are different sub-grid-scale (SGS) stress models [9-12] for closuring of filtered equations. The most popular SGS model is the Smagorinsky eddy-viscosity model. The aim of this study is the evaluation of LES with respect to RANS approach in the prediction of flame characteristics in MILD combustion.

The Numerical Set-up

The numerical model constructed for this study is based on the geometry and dimensions of the experimental JHC burner used by Dally et al. [1]. The experimental burner consists of an insulated and cooled central jet (i.d. = 4.25 mm) and an annulus (i.d.= 82 mm) with a secondary burner mounted upstream of the exit plane. The secondary burner provides hot combustion products which are mixed with air and nitrogen via two side inlets at the bottom of the annulus to control the O2 levels in the mixture. The cold mixture of air and nitrogen also assists in cooling the secondary burner. The cold mixture of air and nitrogen is composed of 23% O2 and 77% N2 (mass basis). Mean inlet velocities of hot co-flow and wind tunnel air are fixed on 3.2 m/s and mean inlet velocity in fuel jet is 58 m/s. Table 1 lists the experimental conditions that are modelled in this study. The fuel jet mixture consists of 80% methane and 20% hydrogen (mass basis). The computational domain started at the exit plane of the burner. It extended 400 mm downstream in the axial direction and 170 mm in radial direction. An unstructured mesh was generated to discretize the computational domain. The mesh that is used in our simulations involved 1195025 cells. Fig. 1 shows the 3-demensional geometry of the combustion chamber.

Table 1. Operating conditions for cases studied in [1].

Oxidant coflow				T_{fuel}	$T_{hot\ co\text{-}flow}$	$T_{shroud\ air}$
Y_{O2}%	Y_{CO2}%	Y_{N2}%	Y_{H2O}%	305k	1300k	294k
9	5.5	79	6.5			

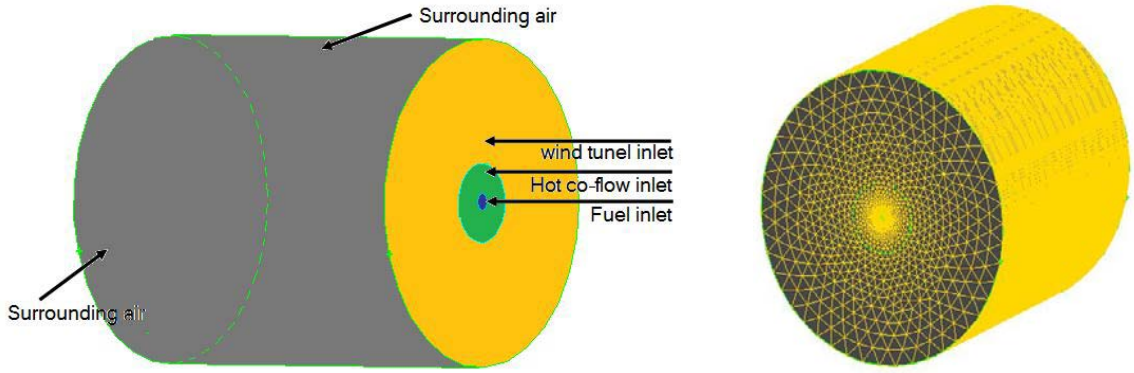

Figure 1. 3D view of the computational domain and boundary conditions.

The numerical simulation of the flow field includes the solution of the governing equations which consists of continuity, momentum, energy, and species conservation which are averaged and filtered by two methods (RANS and LES approaches). For this study, C++ library Open Foam was utilized for numerical solution. This main flow solver in OpenFoam is based on the PISO algorithm [13]. Boundary conditions at upstream are set as velocity profiles, inlet temperature, species, and mass fractions. The velocity profiles at the inlets are assumed to be uniform. In this paper, a simple reaction mechanism, one step for CH_4 and one step for H_2, is used for mixture of CH_4/H_2 which is shown as follows [14, 15],

$CH_4 + 2O_2 => CO_2$
$H_2 + 0.5O_2 => H_2O$

The LES Governing Equations and SGS Model

The filtered continuity, momentum, species and energy equations for LES are expressed as [16, 17],

$$\frac{\partial \overline{\rho}}{\partial t} + \frac{\partial}{\partial x_i}\left(\overline{\rho}\widetilde{u}_i\right) = 0. \tag{1}$$

$$\frac{\partial \overline{\rho}\widetilde{Y}_k}{\partial t} + \frac{\partial}{\partial x_i}\left(\overline{\rho}\widetilde{u}_i\widetilde{Y}_k\right) = \frac{\partial}{\partial x_i}\left(\mu\frac{\partial \widetilde{Y}_k}{\partial x_i} - \overline{\rho}\left(\overline{u_i Y_k} - \widetilde{u}_i\widetilde{Y}_k\right)\right) + \overline{\dot{\omega}}_k \qquad k = 1,\ldots,N. \tag{2}$$

$$\frac{\partial \overline{\rho}\widetilde{u}_i}{\partial t} + \frac{\partial}{\partial x_i}\left(\overline{\rho}\widetilde{u}_i\widetilde{u}_j\right) + \frac{\partial \overline{p}}{\partial x_j} = \frac{\partial}{\partial x_i}\left(\overline{\tau}_{ij} - \overline{\rho}\left(\overline{u_i u_j} - \widetilde{u}_i\widetilde{u}_j\right)\right) + \overline{\rho}g. \tag{3}$$

$$\frac{\partial \overline{\rho}\widetilde{h}}{\partial t} + \frac{\partial}{\partial x_i}\left(\overline{\rho}\widetilde{u}_i\widetilde{h}\right) = \frac{\overline{Dp}}{Dt} + \frac{\partial}{\partial x_i}\left(\frac{\mu}{\Pr}\frac{\partial \overline{h}}{\partial x_i} - \overline{\rho}\left(\overline{u_i h} - \widetilde{u}_i\widetilde{h}\right)\right). \tag{4}$$

In Eq. 2, the thermal diffusion (Soret effect) and the pressure diffusion are neglected. In this work it is assumed that Sc_k (Schmidt number) is unity which means that the effective specie diffusivity is equal to the viscosity. In Eq. 4, h, the enthalpy consists of sensible enthalpy and enthalpy of formation. Moreover, the results of Christo and Dally [4, 5] demonstrated that for

the JHC configuration, thermal radiation did not have noticeable effect on the results; so, the thermal radiation is ignored in this study. In addition, it is assumed that Lewis number is equal to unity. Generally, in the LES equations, the sub-grid-scale stress τ_{ij} is defined by,

$$\tau_{ij} = \bar{\rho}\left(\overline{u_i u_j} - \tilde{u}_i \tilde{u}_j\right). \tag{5}$$

For the SGS stress, the Smagorinsky models is adopted, which gives [16, 17],

$$\tau_{ij} - \frac{\delta_{ij}}{3}\tau_{kk} = -2\mu_{SGS}\bar{S}_{ij}, \qquad \bar{S}_{ij} = \frac{1}{2}\left(\frac{\partial \bar{u}_i}{\partial x_j} + \frac{\partial \bar{u}_j}{\partial x_i}\right), \qquad \mu_{SGS} = \bar{\rho} C_k \sqrt{k}\Delta, \qquad \tau_{kk} = 2\bar{\rho}k. \tag{6}$$

Where Δ is the filter size computed from $\Delta = \sqrt[3]{\Delta x \Delta y \Delta z}$; also, k is computed by,

$$\sum_i \sum_j \bar{\rho}\bar{S}_{ij}\tau_{ij} + \frac{C_e \bar{\rho} k^{3/2}}{\Delta} = 0. \tag{7}$$

In the above equations, C_k and C_e are 0.02 and 1.048, respectively. The sub-grid scale mass flux and heat flux are closed by gradient modeling as,

$$\bar{\rho}\left(\overline{u_i Y_k} - \tilde{u}_i \tilde{Y}_k\right) = -\frac{\mu_{SGS}}{Sc_t}\frac{\partial \tilde{Y}}{\partial x_i}, \qquad \bar{\rho}\left(\overline{u_i h} - \tilde{u}_i \tilde{h}\right) = -\frac{\mu_{SGS}}{\mathrm{Pr}_t}\frac{\partial \tilde{h}}{\partial x_i}. \tag{8}$$

Where Sc_t and Pr_t are model constants, $Sc_t = Pr_t = 1.0$.

The RANS Governing Equations and Standard k-ε Model

Balance equations for the mean quantities in RANS simulations are obtained by averaging the instantaneous governing equations. This averaging procedure introduces unclosed quantities that have to be modelled by turbulence models. Using the Favre averages formalism, the averaged balance equations become [16, 17]:

$$\begin{aligned}
&\frac{\partial \bar{\rho}}{\partial t} + \frac{\partial}{\partial x_i}\left(\bar{\rho}\tilde{u}_i\right) = 0. \\
&\frac{\partial \bar{\rho}\tilde{u}_i}{\partial t} + \frac{\partial}{\partial x_i}\left(\bar{\rho}\tilde{u}_i\tilde{u}_j\right) + \frac{\partial \bar{p}}{\partial x_j} = \frac{\partial}{\partial x_i}\left(\bar{\tau}_{ij} - \bar{\rho}\overline{u_i'' u_j''}\right) + \bar{\rho}g. \\
&\frac{\partial \bar{\rho}\tilde{Y}_k}{\partial t} + \frac{\partial}{\partial x_i}\left(\bar{\rho}\tilde{u}_i\tilde{Y}_k\right) = \frac{\partial}{\partial x_i}\left(\mu\frac{\partial \tilde{Y}_k}{\partial x_i} - \bar{\rho}\overline{u_i'' Y_k''}\right) + \bar{\dot{\omega}}_k \qquad k = 1,\ldots,N. \\
&\frac{\partial \bar{\rho}\tilde{h}}{\partial t} + \frac{\partial}{\partial x_i}\left(\bar{\rho}\tilde{u}_i\tilde{h}\right) = \frac{\overline{Dp}}{Dt} + \frac{\partial}{\partial x_i}\left(\frac{\mu}{\mathrm{Pr}}\frac{\partial \bar{h}}{\partial x_i} - \bar{\rho}\overline{u_i'' h''}\right).
\end{aligned} \tag{9}$$

Closure for the Reynolds stress terms in the government equations were achieved using the *k*–*ε* turbulence model. Dally [5] showed that the standard k-ε model with a modified constant $C_{\varepsilon 1}$ from 1.44 to 1.6 in the dissipation rate equation is the best model among different k-ε models for numerical simulation of MILD combustion. Therefore, it is used as the RANS

model in this study. In Eq. 9, $\overline{\rho}\widetilde{u_i''Y_k''}$ and $\overline{\rho}\widetilde{u_i''h''}$ are closed using a classical gradient assumption,

$$\overline{\rho}\widetilde{u_i''Y''} = -\frac{\mu_t}{Sc_{kt}}\frac{\partial \widetilde{Y}_k}{\partial x_i}, \qquad \overline{\rho}\widetilde{u_i''h''} = -\frac{\mu_t}{\mathrm{Pr}_t}\frac{\partial \widetilde{h}}{\partial x_i}. \tag{10}$$

It is also assumed that Sc_{kt} (turbulent Schmidt number), and Pr_t (turbulent Prandtl number) are unity. The turbulent viscosity is estimated as:

$$\mu_t = \overline{\rho} C_\mu \frac{k^2}{\varepsilon}. \tag{11}$$

Following the turbulence viscosity model proposed by Boussinesq, the turbulent Reynolds stresses $\overline{\rho}\widetilde{u_i''u_j''}$ are described using the viscous tensor τ_{ij} expression that is obtained for Newtonian fluids.

$$\overline{\rho u_i''u_j''} = \overline{\rho}\widetilde{u_i''u_j''} = -\mu_t\left(\frac{\partial \widetilde{u}_i}{\partial x_j} + \frac{\partial \widetilde{u}_i}{\partial x_i} - \frac{2}{3}\delta_{ij}\frac{\partial \widetilde{u}_k}{\partial x_k}\right) + \frac{2}{3}\overline{\rho}k. \tag{12}$$

Combustion Model

The Partially Stirred Reactor (PaSR) model is used in this work as the combustion model. In the PaSR approach, a computational cell is split into two different zones: in one zone all reactions occur, while in the other one there are no reactions (Fig. 2). Therefore, the composition changes due to mass exchange with the reacting zone. In addition, the reaction zone is treated as a perfectly stirred reactor (PSR), in which all reactants are assumed to be perfectly mixed with each other. This allows us to neglect any fluctuations when calculating the chemical source terms. Three average concentrations are presented in the reactor, the mean mixture concentration of the feed c^0, the mixture concentration in the reaction zone c, the mixture concentration at the exit of the reactor c^1.

Figure 3. Conceptual diagram of PaSR reactor (the reaction zone is painted) [18].

The whole combustion process could be regarded as two processes. The first is the initial concentration in the reaction zone changes from c^0 to c as it reacts; the second is the reaction mixture c is mixed with the no reaction mixture c^0 by turbulence, the results in the averaged concentration c^1. The reaction rate of this computational cell is determined by the fraction of the reactor in this cell. It seems quite clear that it should be proportional to the ratio of the

chemical reaction time τ_c to the total conversion time in the reactor, i.e. the sum of the micro-mixing time τ_{mix} and reaction time τ_c [8, 18, 19],

$$\kappa_k = \frac{\tau_c}{\tau_c + \tau_{mix}}. \tag{13}$$

The micro-mixing time τ_{mix} characterizes the exchange process between reaction mixture and no reaction mixture. In this paper micro-mixing time was obtained from the k-ε equation, $\tau_{mix}=C_{mix}\sqrt{(\mu+\mu t)/\rho\varepsilon}$, the model constant C_{mix} was set to 1. The reaction time was derived from the laminar reaction rate. Thus, the overall reaction rate $\overline{\dot{\omega}}$ and the homogenous reaction rate $\dot{\omega}$ of this computational cell, which represents the reaction rate of the species according to the used kinetic mechanism, have the following relationship,

$$\frac{c^1{}_k - c_k{}^0}{dt} = \overline{\dot{\omega}_k} = k_k \dot{\omega}_k. \tag{14}$$

Results and Discussions

Fig. 2 illustrates the instantaneous temperature and CH4 mole fraction maps which are obtained using the LES method. In this figure, it is seen that, far from the jet exit, the turbulence is much higher. This fact, increasing turbulence, is also depicted in Fig. 3, where the fluctuation of H2O concentration is shown along the flame.

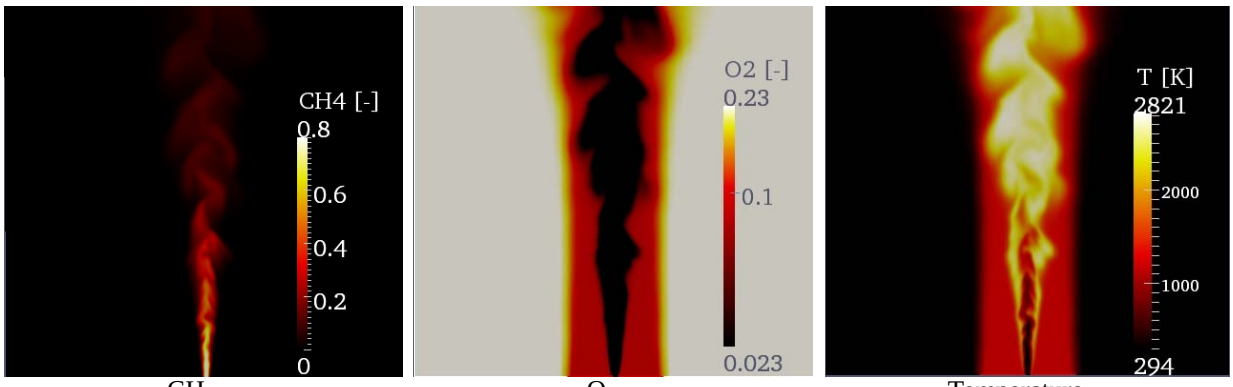

CH_4 O_2 Temperature

Figure 2. Predicted instantaneous temperature and species profiles on the centre plane of the combustion Chamber using LES.

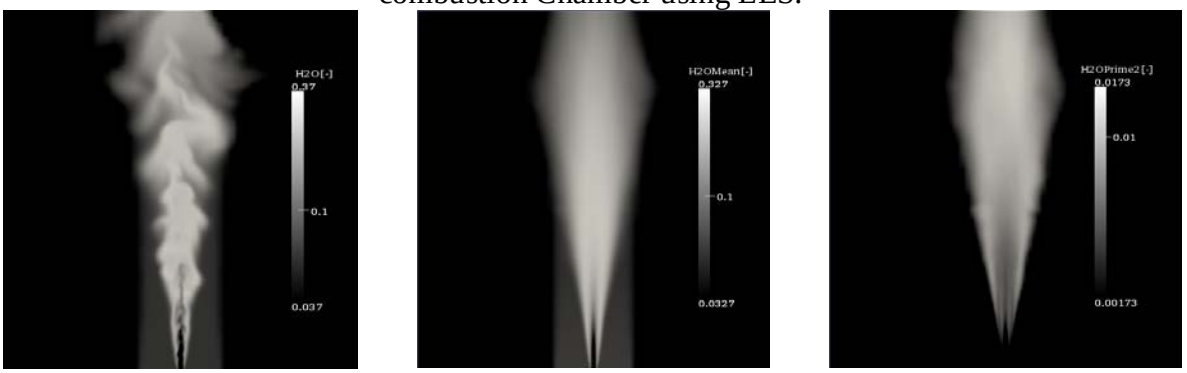

Figure 3. Profiles for instantaneous and Mean H_2O, and H_2O fluctuation on the centre plane of the combustion Chamber using LES.

The contour of CH_4 in Fig. 2 shows that the fuel vortex size is increased when moving farther from the jet exit. The large fuel vortexes cause the fuel mix with oxygen that comes from wind tunnel (where O_2 mass fraction is 23%). This condition is not suitable for MILD combustion. In far distances from the fuel inlet, the flame temperature is much higher than the temperature near the inlet. One reason for this temperature rise is the appearance of highly turbulent and wrinkled flame, far from the nozzle. The increase of flame surface and turbulence intensity promotes the mixing rate of fuel with high-Oxygenized oxidizer, which, in turns, intensifies the burning rate and the energy release.

Fig. 4 shows the temperature contours in different locations along the jet axis. Part (a) in Fig. 4 corresponds to a simulation using LES, while part (b) in Fig. 4 shows the temperature contours obtained utilizing the RANS approach. It is observed that a symmetric flame is obtained by the RANS simulation of the MILD flame (see Fig. 4-b). On the other hand, contours of part (a) reveals that the LES modeling predicts an asymmetric flame far from the inlet. There has been a large discrepancy between the MILD flame temperature obtained using the k-ε model with the experimental measurement of Dally (for example in 7, 13). The past simulations not only used (at the best) the k-ε model, they were based on two-dimensional axi-symmetric geometry, to simulate the Dally experiment symmetric setup. The present LES modeling, that is in essence a three dimensional approach, reveals that the true MILD flame field in Dally setup is a three-dimensional phenomenon. This difference can be a reason behind the above mentioned temperature discrepancy.

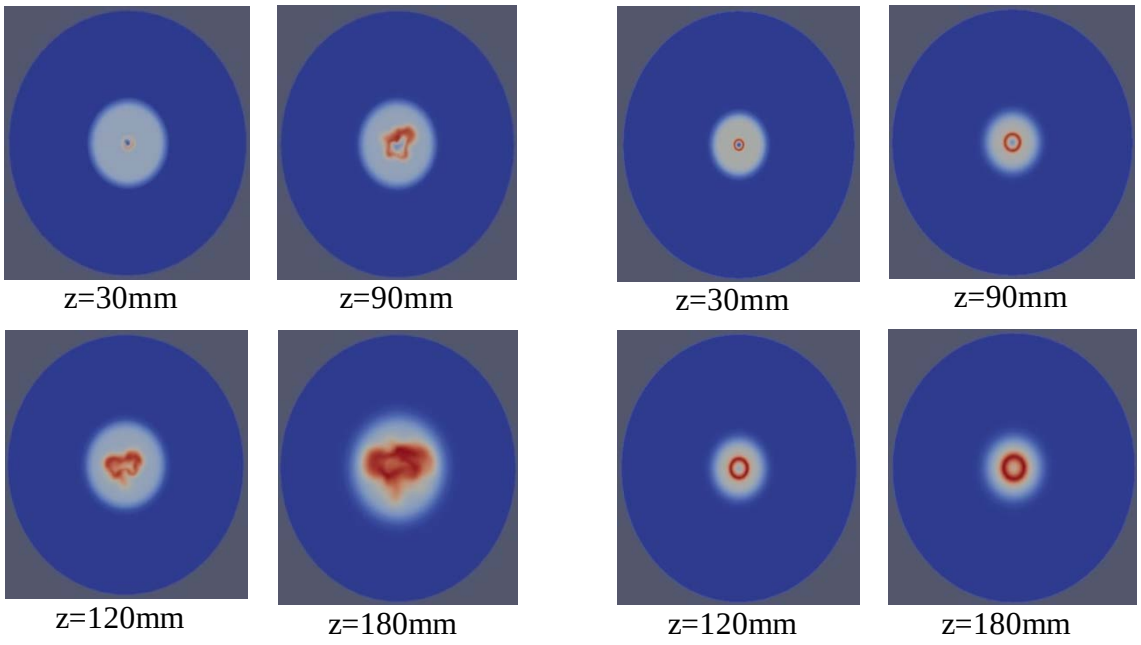

a) Instantaneous temperature contour using LES.

b) Temperature contour using k-ε method.

Figure 4. Temperature contour in different locations.

To further clarify this fact, the radial temperature profile inside the flame, in axial location 30 mm from the fuel nozzle, is shown in Fig. 5. It is observed that the temperature profile predicted by LES modeling is much closer to the experimental values than the data obtained by the k-ε model.

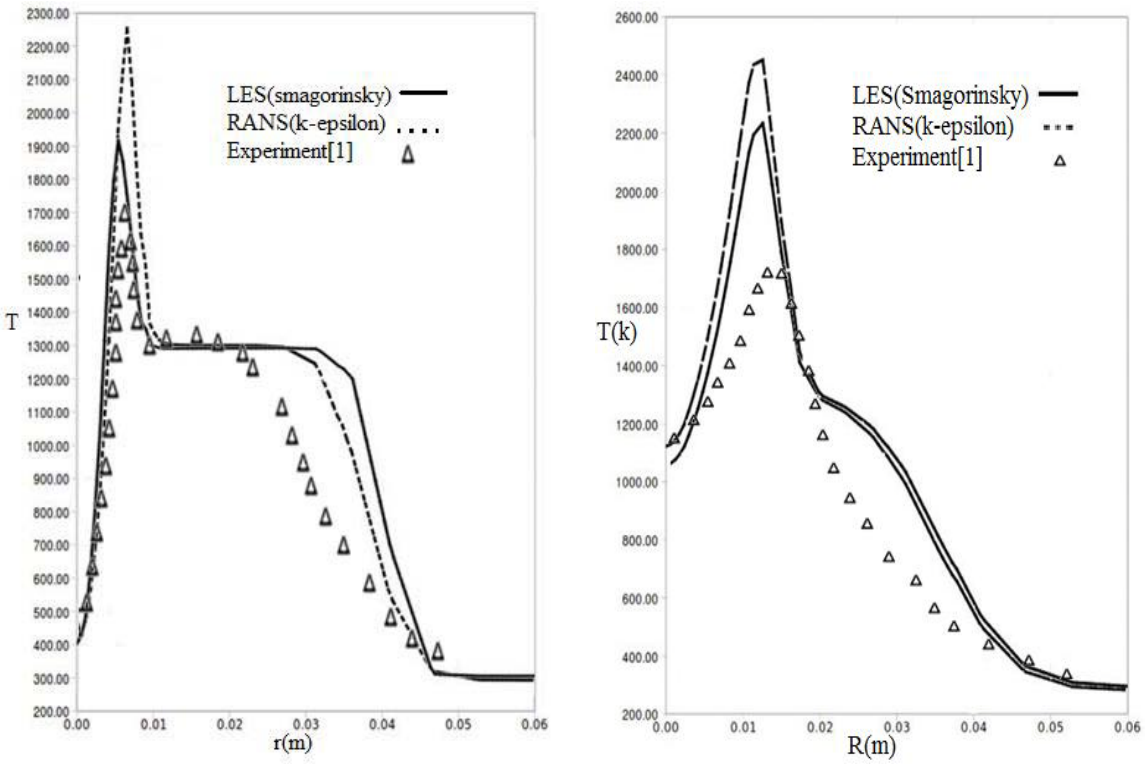

Z=30mm Z=120mm

Figure 5. Comparison of radial distribution of temperature profile obtained from LES and k- ε methods with experimental results[1].

There is still some difference between the LES prediction with experimental temperature. Experimental value of maximum temperature in axial location z=30 mm is 1700 Kelvin while the maximum temperature predicted by the LES technique is 1900 Kelvin (and 2270kelvin by the k-ε method). Moreover, far from the nozzle exit (z=120mm), the LES predicts temperature and species better than the RANS approach. The maximum temperature predicted by the LES is 2200 Kelvin while the RANS method predicts it approximately 2500 Kelvin (experimental value of maximum temperature at z=120 mm is 1700 Kelvin.)
This difference is attributed to the present simulations Kinetic modeling. Due to very high computational cost of LES modeling, a simple two-step kinetic is used in this study. It is predicted that the difference between experimental data and the simulation prediction will be further reduced if a better kinetic model is used.

Conclusion

In this work, a numerical study of JHC flame of Dally has been performed. The results show that the accuracy of numerical solution highly depends on the turbulent model. It is found that the LES modeling predict the characteristics of MILD combustion much better than the RANS approach. It is shown that the axi-symmetric assumption of MILD flame field in Dally experimental setup is not correct far from the jet exit. The LES modeling, unlike the RANS method, predicts an asymmetric MILD flame. The difference in the prediction of the flame topology is suggested as one of the reason of different predictions of two turbulence modeling approaches.

Nomenclature

ρ	density
u_i	velocity in i-direction
g	gravity
p	pressure
Y_k	mass fraction of species k
h	enthalpy
T	temperature
c_k	Concentration for species k
τ_{ij}	viscous tensor
μ	dynamic viscosity
Sc_k	Schmidt number for species k
$\dot{\omega}_k$	mass reaction rate of species k per unit volume
Pr	Prandtl number
μ_{SGS}	subgrid scale viscosity
μ_t	the turbulent viscosity
Δ	filter size
Pr_t	turbulent Prandtl number
Sc_{tk}	turbulent Schmidt number for species k
k	turbulent kinetic energy
ε	kinetic energy dissipation rate
κ_k	reactive fraction of species k
S_{ij}	Strain rate

References

[1]. Dally, B.B., Karretis, A.N., Barlow, R.S., "Structure of Turbulent Non-Premixed Jet Flameless in a Diluted Hot Coflow", Proc. Comb. Inst. 29:1147-1154 (2002).

[2]. Wunning, J.G., "Flameless combustion in thermal process technology", 2nd International Seminar on High Temperature Combustion, Stockholm, Sweden, 2000.

[3]. Cavaliere, A., Joannon, M.D., "MILD Combustion", Progress in Energy and Combustion Science, 30: 329-366, 2004.

[4]. Christo, F.C., Dally, B.B., "Application of Transport PDF Approach for Modeling MILD Combustion", 15th Australasian Fluid Mechanics Conference, Sydney, Australia, 2004.

[5]. Christo, F.C., Dally, B.B., "Modeling Turbulent Reacting Jets Issuing into a Hot and Diluted Coflow", Combustion and Flame 142:117-129 (2005).

[6]. Galletti, C., Parente, A., Tognotti, L., "Numerical and experimental investigation of a mild combustion burner", Combustion and Flame **151**(4): 649-664 (2007).

[7]. Golovitchev, V.I., Nordin, N., Jarnicki, R., Chomiak, J., "3-D Diesel Spray Simulations Using a New Detailed Chemistry Turbulent Combustion Model", CEC/SAE Spring Fuels & Lubricants Meeting & Exposition, Paris, FRANC, 2000.

[8]. Golovitchec, V.I., Chomiak, J., "Numerical Modeling of high temperature air Flameless combustion", the 4th international symposium on high temperature air combustion and gasification, Rome, Italy, 2001.

[9]. Zhou, L.X., Hu, L.Y., Wang, F., "Large-eddy simulation of turbulent combustion using different combustion models", Fuel 87: 3123–3131 (2008).

[10]. Mahesh, K., Constantinescu, G., Apte, S., Iaccarino, G., Ham, F., Moin, P., "Large-Eddy Simulation of Reacting Turbulent Flows in Complex Geometries", Journal of Applied Mechanics 73: 374-381 (2006).

[11]. Fureby, C., Tabor, G., Weller, H.G., Gosman, A.D., "A comparative study of subgrid scale models in homogeneous isotropic turbulence", Physics of Fluids 9: 1416-1429 (1997).

[12]. Fureby, C., “On subgrid scale modeling in large eddy simulations of compressible fluid flow”, Physics of Fluids 8: 1301-1311 (1996).
[13]. OpenFOAM, OpenFoam user guide, version1.5, 9th Edition, 2008.
[14]. Turns, S.R., “An Introduction to Combustion”, second ed. McGraw Hill, 2006.
[15]. Westbrook, C., Drye, F., “Simplified Reaction Mechanisms for the Oxidation of Hydrocarbons Fuels in Flames”, Combustion Science and Technology, 27: 31-43(1981).
[16]. Poines, T., Veynante, D., Theoretical and Numerical Combustion, Second Edition, Edwards, 2005.
[17].http://foam.sourceforge.net/doc/Doxygen/html/classFoam_1_1compressible_1_1turbulenceModel.html.
[18]. Hua, W., Yong-chang, L., Ming-rui, W., Yu-sheng, Z., “Multidimensional modeling of Dimethyl Ether (DME) spray combustion in DI diesel engine”, Journal of Zhejiang University SCIENCE, 4:276-282 (2005).
[19]. D’Errico, G., Ettorre, D., Lucchini, T., “Comparison of Combustion and Pollutant Emission Models for Dl Diesel Engines”, International conference on internal combustion engine, Napoli, Italy, 2007.